Effect of Support Material on MgO-Based Catalyst for Production of New Hydrocarbon Bio-Diesel

Paweesuda Natewong[a]*, Yayoi Murakami[b], Haruki Tani[c], Kenji Asami[d]

[a,d]*Faculty of Environmental Engineering, The University of Kitakyushu, Kitakyushu 808-0135, Japan*

[b]*HiBD Research Institute, The University of Kitakyushu, Kitakyushu 808-0135, Japan*

[c]*Graduate of School of Engineering, Nagoya University, Nagoya 464-8601, Japan*

[a]*Email: u3daa401@eng.kitakyu-u.ac.jp*

[b]*Email: yayoi-murakami@env.kitakyu-u.ac.jp*

[c]*Email: h-tani@numse.nagoya-u.ac.jp*

[d]*Email: asami@kitakyu-u.ac.jp*

Abstract

The catalytic-decarboxylation of waste cooking oil was carried out over 10wt% MgO catalysts supported on different supports, γ-Al_2O_3, ZrO_2, SiO_2 and active carbon. The prepared catalysts were characterized by BET, XRD, FE-SEM and TGA. The results of XRD and BET indicated that the obtained catalysts were highly dispersion on the support with large specific surface area. The catalytic-decarboxylation performance of catalysts was investigated by the CO_2 yield and carried out in an agitated reactor under inert gas for 7 h at 430 °C. The triglycerides in waste cooking oil were converted into a mixture of hydrocarbons, CO, CO_2 and water by breaking C-C and C-O bonds by direct decarboxylation and subsequent cracking. The supported MgO-based catalysts showed high catalytic activity and could convert triglycerides to long chain hydrocarbons in diesel specification range (C_{10}-C_{20}). In the case of 10M/AC catalyst, the addition of ZrO_2 exhibited an inhibitor the coke formation on the catalyst surface, due to surface oxygen vacancies, which help gasify the carbon that deposit on the surface of the catalyst.

Keywords: High quality Bio-diesel; Deoxygenation; Decarboxylation; Support material.

----

* Corresponding author.

1. Introduction

Biodiesel is renewable and clean-burning fuel that is made through a chemical process which converts vegetable oils or animal fats into fatty acid methyl esters (FAME)[1]. However, the high oxygen content in the ester component limits their application for vehicle fuels due to their unfavorable cold flow properties (CFPP-cold filter plugging point: >25 °C) and poor storage (oxidation and heat) stability of fatty acid esters[2,3]. Therefore, increasing attentions have moved towards catalytic deoxygenation processes in which oxygen is eliminated mostly as H_2O or CO_x. Of these deoxygenation methods, hydrodeoxygenation (HDO) via hydrotreating catalysts such as NiMo and CoMo-based sulfide catalysts are normally used to convert vegetable oils to liquid hydrocarbon[4-6]. On the other hand, the requirement of hydrogen is the main drawback of this method as well as sulfide catalysts which can contaminate the products and become deactivated in the presence of water.

In view of this, alternative method in which deoxygenation is achieved by decarboxylation of fatty acids or derivatives have been reported[7-19]. In decarboxylation, the hydrocarbon chain in fatty acid is inert towards catalyst surface, whereas the carboxylic group is adsorbed on the catalyst surface resulting in the removal of the carboxylic group through C-C cleavages to release CO_2 (and possibly carbonyl group through C-C and C-O cleavages to release CO), thereby the formation of hydrocarbon production exhibited one carbon less than the original fatty acid chain. The most active catalysts such as Pd, Pt and Rh were found to be effective in catalyzing the deoxygenation reaction [20,21]. However, the high cost of these noble metals represents an important drawback from an economic standpoint, which leads to search for a cheaper catalyst. In previous work we have demonstrated that a typical basic metallic oxide, MgO displayed near performance comparable with precious metal catalyst in the upgrading of triglycerides and fatty acids to hydrocarbons[22-24]. Zhang et al. [25] investigated the decarboxylation of aromatic acids using naphthoic acid over series of alkaline-earth metal oxides such as CaO, MgO, SrO, and BaO. All of these oxides showed high catalytic activity in naphthoic acid conversion by 55 to 95%. CO_2 formation was observed only in magnesium oxide, yielding 18%. In spite these promising results, MgO exhibits a poor CO_2 adsorption capacity due to its low surface area and pore volume. As a result, many studies were conducted to improve the activity of MgO. It is well known that the supports could be improved the performance of the catalysts since the major roles of them are to prepare and preserve the capability to stabilize metal particles against thermal sintering as well as well-dispersed catalytic phases during the reaction. In literature, the high surface area supports are widely often used to enhance the activity for various catalysts such as γ-alumina, silica, active carbon, cerium oxide and zirconia. CeO_2 and ZrO_2 have proved to be catalyst supports with high oxygen storage capability which would improve catalytic performance and solve sintering problem of MgO catalysts.

Therefore, the aim of this work is to investigate the influence of the nature of support, namely γ-Al_2O_3, SiO_2, ZrO_2 and AC on catalytic performance of magnesium oxide in the catalytic cracking-decarboxylation of waste cooking oil.

2. Experimental

2.1   Catalyst preparation

The magnesium oxide catalysts supported on different supports were prepared by the incipient wetness impregnation method, with aqueous solution of magnesium nitrate hexahydrate (Mg(NO$_3$)$_2$.6H$_2$O, 99.0% purity, Wako, Japan). A commercial γ-alumina (S$_{BET}$ = 225 m^2/g and PV = 0.494 cm^3/g), silica (S$_{BET}$ = 259 m^2/g and PV = 1.02 cm^3/g), zirconium oxide (S$_{BET}$ = 15 m^2/g and PV = 0.01 cm^3/g) and active carbon (S$_{BET}$ = 813 m^2/g and PV = 0.638 cm^3/g) were used as the supports in this study. The supports were initially dried at 110 °C overnight to remove adsorbed moisture. Magnesium nitrate hexahydrate was dissolved in the deionized water and then added dropwise into the supports. After the impregnation, the impregnated samples were evaporated at 40 °C and then dried in an oven at 110 °C overnight followed by calcined at 500 °C for 3 h. The total MgO loading was 10wt% for all of the supports. The catalysts were denoted as 10M/Al$_2$O$_3$, 10M/SiO$_2$, 10M/ZrO$_2$ and 10M/AC.

2.2   Catalyst characterization

The specific surface area, pore volume and pore diameter of the fresh and spent catalysts were determined by N$_2$ adsorption-desorption measurements using a BELSORP-mini II instrument (Japan Bel Inc.). The spent catalysts were heated at 250 °C for 3 h to remove any trace oils that may have accumulated on the catalyst pores. Before analyzing, the catalysts were degassed at 200 °C for 2 h in order to remove the moisture adsorbed on the surface. Catalyst surface area was calculated using the Brunauer, Emmett and Teller (BET) method, total pore volume was determined by measuring the volume of adsorbed gas at a *P/P$_0$* of 0.99, and pore size distribution were obtained using the Barrett-Joyner-Halenda (BJH) method. The powder X-ray diffraction (XRD) patterns of the fresh and spent catalysts were obtained using a RIGAKU, XRD-DSC-XII diffractometer via CuKα as the radiation source (λ = 1.54 Å) at running conditions for the X-ray tube 40 kV and 20 mA at room temperature. Diffraction patterns were collected from 10° to 80°. Surface morphologies of both fresh and spent catalysts were performed using a Hitachi S5200 field emission scanning electron microscope (FE-SEM) operated at 20.0 kV. The amount of coke on the spent catalysts was measured using the simultaneous thermogravimetric (TG) and differential thermal analysis (DTA) . Around 5 mg of spent catalyst was placed in a platinum crucible that was introduced in a RIGAKU TG-DTA 8210. The spent sample was heated under air flow (50 mL/min) from room temperature up to 900 °C at heating rate of 10 °C/min.

2.3   Catalyst testing

Reaction experiments for evaluating catalytic performance were performed in an agitated reactor system at 430 °C under atmospheric pressure as shown in **Figure 1**. Catalyst was charged into the reactor and was heated up to 430 °C at the same time of a carrier gas He at a flow rate 50 mL/min. The waste cooking oil was supplied from the university restaurant was fed continuously at a rate 0.25 mL/min. The gaseous products exiting the reactor were cooled and condensed at 0 °C. The uncondensed gaseous products were analyzed every 30 min by a GC-TCD and a GC-FID on line (Shimadzu GC-14A). The liquid trap product was analyzed carbon number distribution by GC-MS (Agilent GC-7980A). Total acid value of the product oil was measured by potentiometric titration methods according to JIS 2501-2003.
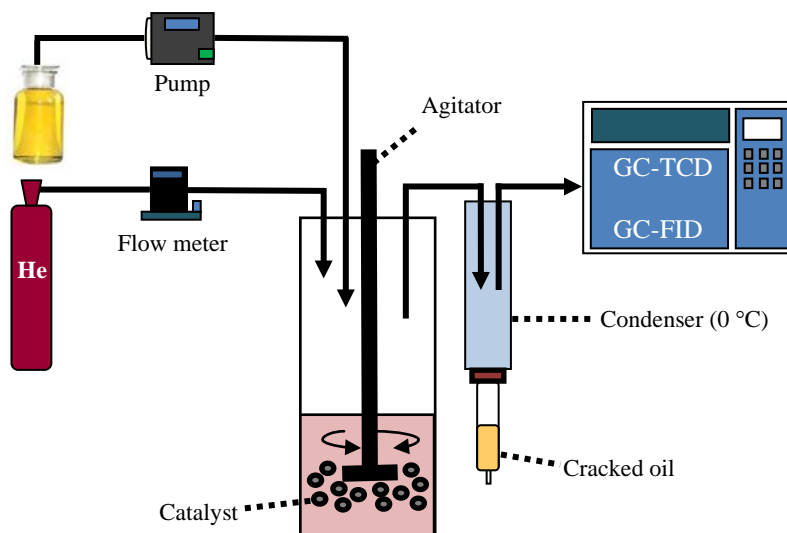
Figure 1: Reaction apparatus for catalytic decarboxylation

The product selectivity could be calculated by using the calculation equation listed below:

Selectivity (C%) = (C ataoms in each product/Sum of C atom in all the product) × 100%   *(1)*

3. Results and discussion

3.1   Catalyst characterization

Table 1: Textural properties of the fresh and spent catalysts

Catalysts	Fresh			Spent		
	S_{BET} (m^2/g)	V_{Total} (cm^3/g)	D_{pore} (nm)	S_{BET} (m^2/g)	V_{Total} (cm^3/g)	D_{pore} (nm)
10M/ZrO$_2$	6	0.04	23.77	23	0.03	4.95
10M/Al$_2$O$_3$	175	0.39	8.96	158	0.20	5.12
10M/SiO$_2$	186	0.14	2.94	185	0.67	14.57
10M/AC	549	0.44	3.21	45	0.05	7.01

The textural properties of the fresh and spent catalysts with different supports evaluated by nitrogen adsorption-desorption are summarized in **Table 1**. It can be observed that the high surface area of 10M/γ-Al$_2$O$_3$, 10M/SiO$_2$ and 10M/AC exhibited higher surface area and pore volume than 10M/ZrO$_2$, due to those of support having high surface area. As for spent catalysts, the surface area and pore volume of the active carbon (AC) which were the highest among the four supports, were decreased dramatically after decarboxy-cracking reaction due to the partial blockage of pores of support by carbon formation over the catalyst and active metal sintering, which was

in agreements with FE-SEM and XRD results. While the surface areas of the alumina and silica supports were preserved. On the other hand, the surface area of zirconium oxide support increased significantly from 6 to 23 m^2/g while their pore volume and pore diameter decrease, may be coke deposit unevenly in catalyst pore wall layer by layer, but to form micropore in macropores or large mesopores via pore-making [26].

In **Figure 2** displays the XRD patterns of the fresh and spent MgO-based catalysts with different supports. The XRD patterns of MgO species were only detectable in $10M/ZrO_2$ catalyst with low intensity diffraction peaks at $2\theta = 42°$ and $62°$. While the XRD patterns of γ-alumina, silica and active carbon supports showed a similar profile with broad diffraction peaks of amorphous phase. The absence of diffraction peaks of MgO in $10M/\gamma$-Al_2O_3, $10M/SiO_2$ and $10M/AC$ ascribed to its very high dispersion throughout the support, with a particle size under the detection limit of XRD technique. This is indicated that the high surface area of γ-alumina, silica and active carbon promote the dispersion of MgO. The XRD patterns of spent catalysts are also shown in **Figure 2**. The XRD patterns of the spent $10M/SiO_2$ catalyst showed only amorphous peak, suggesting that catalytic structure had no change during the catalytic reaction. Although no bulk peak of MgO specie was detected in case of fresh $10MgO/AC$ catalyst, the detection of MgO peaks in spent catalyst as the following diffraction peaks detected at $2\theta = 36°$, $42°$ and $62°$ was confirmed the presence of MgO species in fresh catalyst. The detected diffraction peaks of MgO in spent $10MgO/AC$ catalyst could be related to a strong sintering occurred over MgO after reaction. The low intensity diffraction peaks observed at $2\theta = 38°$, $46°$ and $67°$ in the case of $10M/\gamma$-Al_2O_3 catalyst were assigned to the Al_2O_3 cubic phase which had transformed into a Al_2O_3 with hexagonal type of corundum structure, which was consistent with SEM results.
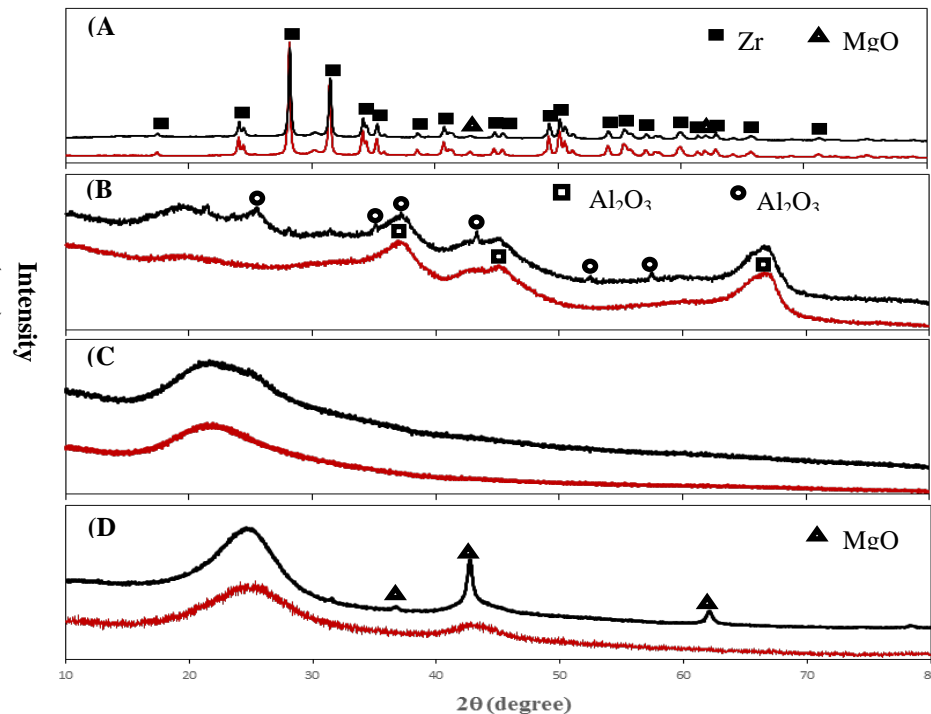
Figure 2: XRD patterns for fresh (Red line) and spent (Black line) catalysts with different supporting (A) $10M/ZrO_2$, (B) $10M/Al_2O_3$, (C) $10M/SiO_2$ and (D) $10M/AC$.

Fresh   Spent
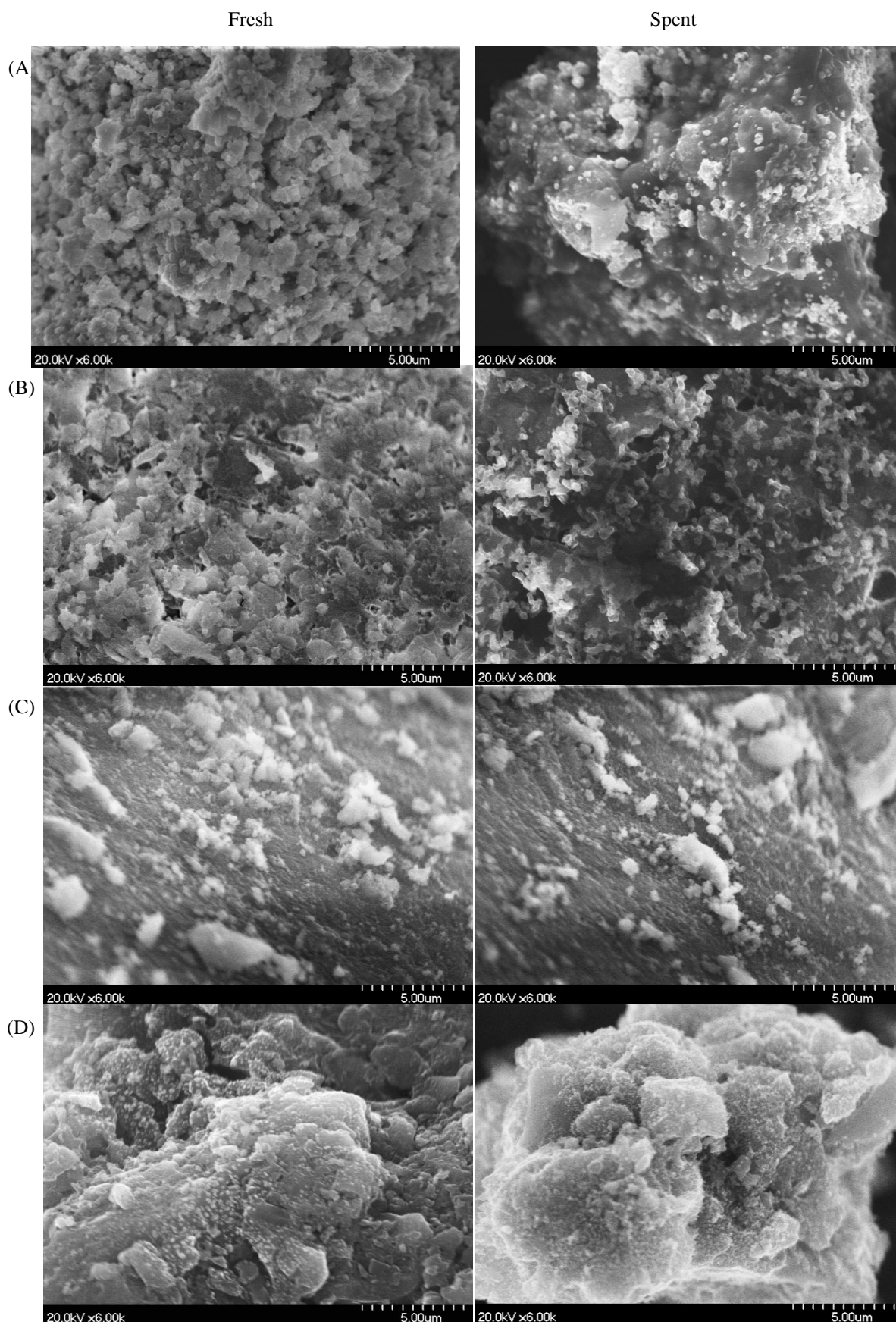
Figure 3: FE-SEM images of fresh and spent catalysts (A) 10M/ZrO$_2$, (B) 10M/Al$_2$O$_3$, (C) 10M/SiO$_2$ and (D) 10M/AC.

Figure 3 shows the morphology of the fresh and spent catalyst surfaces applying FE-SEM analysis. As for the fresh catalysts, a large crystallite of $10M/ZrO_2$ is evident in **Figure 3(A)** due to low surface area. In **Figure 3(B)** shows a kind of a non-uniformity of γ-Al_2O_3. On the other hand, the small dispersion of MgO on the supports was observed in **Figure 3(C-D)**. The $10M/SiO_2$ catalyst exhibited undefined shape of magnesium oxide, while uniform distribution of MgO particles was observed 10M/AC catalyst. As for the reacted catalysts, it can be clearly seen that the morphology of $10M/Al_2O_3$, 10M/AC and$10M/ZrO_2$ catalysts changed significantly after the decarboxylation reaction. For $10M/ZrO_2$ catalyst, large deposits of amorphous were observed.

This heavy carbon formation on the$10M/ZrO_2$ catalyst can be attributed to its structure which was low surface area and large MgO particles. In addition, some hexagonal phase and agglomeration had been found for $10M/Al_2O_3$. On the contrary, there were no significant differences in the morphology changes between the fresh and spent catalysts observed for the $10M/SiO_2$ catalyst. Spent 10M/AC catalyst was seriously covered by deposited the whisker carbon formed on the surface of the catalyst. This is in line with BET results since surface area of 10M/AC decreased dramatically after reaction.

Figure 4 shows the TGA profile of the spent $10M/Al_2O_3$ catalyst (after 7 h catalytic decarboxylation reaction). The weight loss started at 320-480 °C. The weight loss in this temperature range could be attributed to the combustion of the high molecular weight derived from waste cooking oil. The peak of coke deposit on all of the spent catalysts was observed at temperature above 480 °C, indicating the strongly coke deposit.

The amount of coke deposit on the spent catalysts is illustrated in **Table 2**. It was found that the coke amount significantly depended on the type of support. This result suggested that two catalysts supported on SiO_2 and ZrO_2 produced less coke compared with the catalysts supported on Al_2O_3 and AC. The highest level of coke was formed on active carbon support, approximately 38.1%. Since the problem of coking was greatest on active carbon to find ways of reducing coking on this material.

It was found that ZrO_2 inhibited the coking due to its mobile oxygen species, which help gasify the carbon that deposit on the surface of the catalyst.

Table 2: Amount of coke deposit

Catalysts	Coke deposit (%)
$10M/ZrO_2$	8.87
$10M/Al_2O_3$	16.4
$10M/SiO_2$	8.76
10M/AC	38.1
5M10Z/AC	15.8
5M20Z/AC	13.9
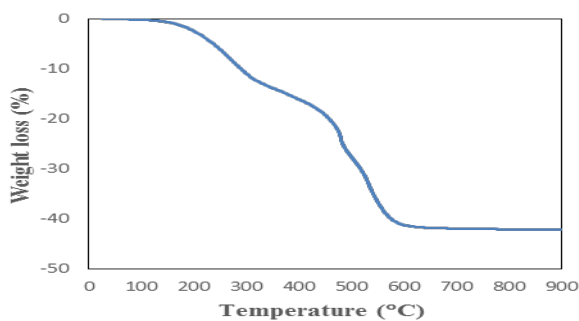
Figure 4: Weight losses determined by TGA analysis of the spent catalyst after catalytic decarboxylation of waste cooking oil

3.2 Catalyst performance

Catalytic activity of the MgO-based catalysts with different supports and %ZrO_2 loading in the catalytic cracking decarboxylation reaction was carried out using an agitated reactor. The finding results are included in **Table 3**. The major products from this reaction were a mixture of liquid hydrocarbons, dry gas (C_1-C_4 hydrocarbons), CO, CO_2, water and residue. According to the results, **Scheme 1** displays the probable pathway for the catalytic cracking-decarboxylation of triglycerides as follows: triglyceride molecules in waste cooking oil have been primarily hydrolyzed to produce 1 mol of glycerine and 3 moles of free fatty acids. The glycerol can be converted to gaseous hydrocarbons and water by dehydration. While, fatty acid would be cracked into hydrocarbons by breaking of the C-C and C-O bonds follows two competitive routes: (1) direct decarboxylation (-CO_2) reaction followed by C-C bond cleavage of the resulting hydrocarbon radicals or (2): C-C and C-O cleavages within the hydrocarbon section of the oxygenated hydrocarbon molecule followed by decarboxylation and decarbonylation of the resulting short chain molecule. These reactions finally yield CO, CO_2 and water as main oxygenated compounds and a mixture of hydrocarbons produced by different reactions such as β-scission, hydrogen transfer or isomerization.

Table 3: Material balance of waste cooking oil by decarboxy-cracking reaction

Catalysts	Product yield (wt%)					
	Cracked oil	Dry gas	CO	CO_2	H_2O	Residue
10M/ZrO_2	69.8	4.8	1.4	5.5	3.0	8.8
10M/Al_2O_3	62.2	6.1	0.7	5.3	3.9	9.9
10M/SiO_2	63.3	9.3	0.6	3.7	6.4	8.4
10M/AC	64.8	4.1	1.0	5.9	4.4	13.4
5M10Z/AC	67.2	2.5	0.6	7.9	4.0	10.2
5M20Z/AC	64.7	5.7	0.8	6.3	4.2	10.0

Reaction conditions: He = 50 ml/min, oil feed flow rate = 0.25 ml/min, reaction temperature 430 °C.
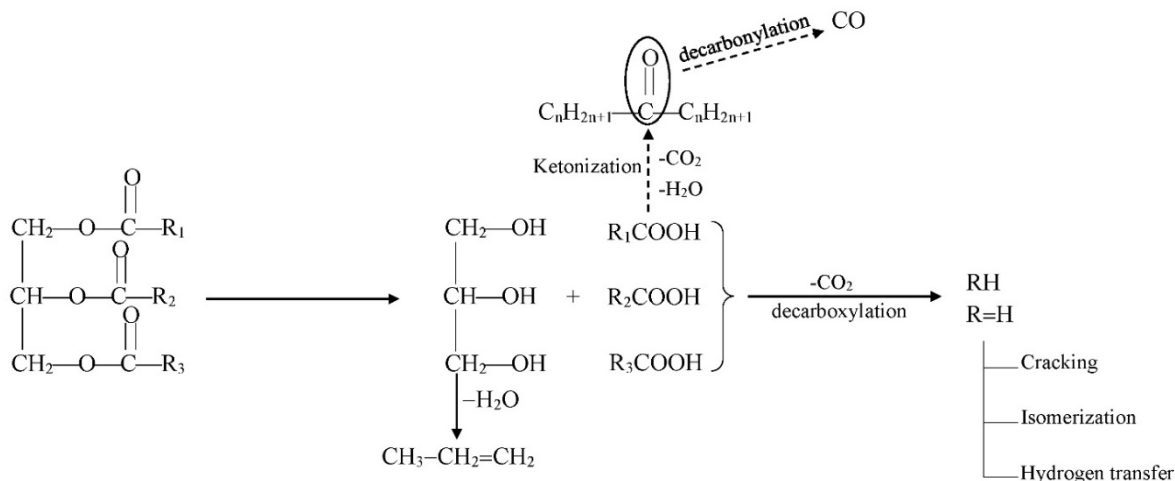
Figure 5-a: Reaction scheme for catalytic decarboxylation of triglycerides to hydrocarbon
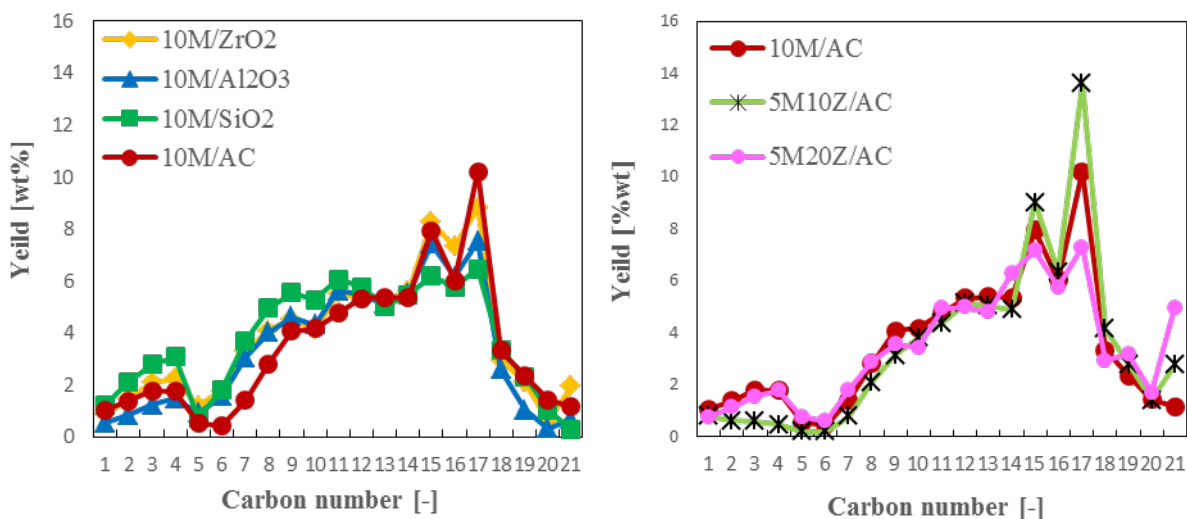
Figure 5-b: Hydrocarbon distribution of the product oils

Figure 5 depicts the hydrocarbon distribution of the product oils. From this result demonstrates that all of catalysts can convert triglycerides to long chain hydrocarbons in diesel specification range (C_{10}-C_{20}) and the C_{17} hydrocarbons were the most abundant compounds after catalytic cracking-decarboxylation reaction. Furthermore, the portion of hydrocarbons with shorter chain in diesel fraction C_{10}-C_{14} were also detected, indicating that the C_{16} and C_{18} fatty acids (mainly consist of palmitic acid group of C_{16} and oleic acid group C_{18}) were converted not only to C_{15} and C_{17} hydrocarbons by direct decarboxylation but also to shorter chain by subsequent cracking reaction. The highest C_{15} and C_{17} yield were observed for the 10M/AC catalyst with 8.1 and 10.2 wt%, respectively. This result revealed that decarboxylation was the main reaction pathway. Whereas the lower yield of C_{17} was observed for 10M/SiO$_2$ and 10M/Al$_2$O$_3$ catalysts. This was mainly due to the fact that the cracking reaction is influenced by the highest acidity of the catalysts. Moreover, in **Figure 6** when focused

on the ratios of C_{16}/C_{15} and C_{18}/C_{17} of 10M/AC catalyst were lower than other catalysts. This indicated that the 10M/AC prefered to decarbonylation/decarboxylation. By the addition of ZrO_2 with 10%wt, it was surprising found that yield of C_{15} and C_{17} increased while ratios of C_{16}/C_{15} and C_{18}/C_{17} decreased, suggesting that the decarboxylation of fatty acid can be greatly promoted by the ZrO_2.
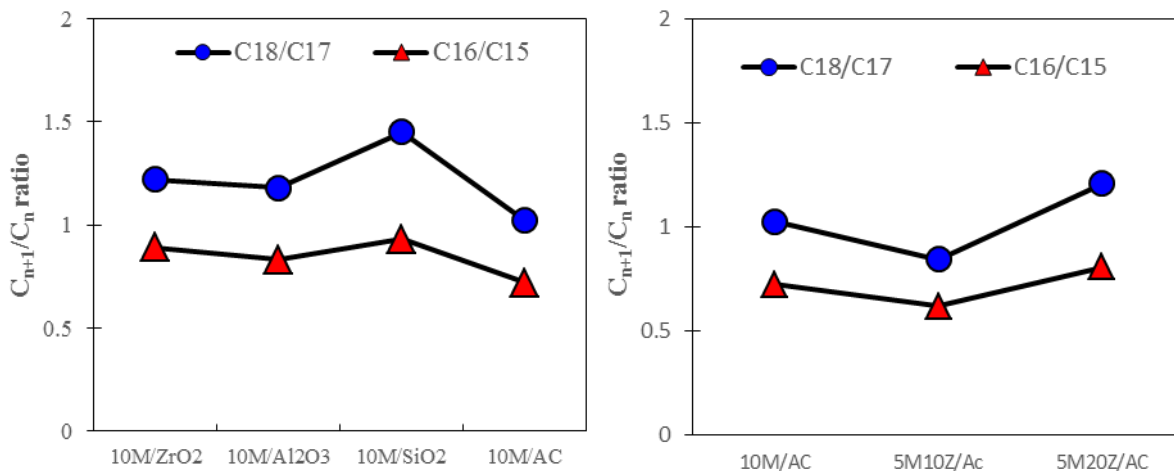
Figure 6: The C_{n+1}/C_n ratio of the product oils
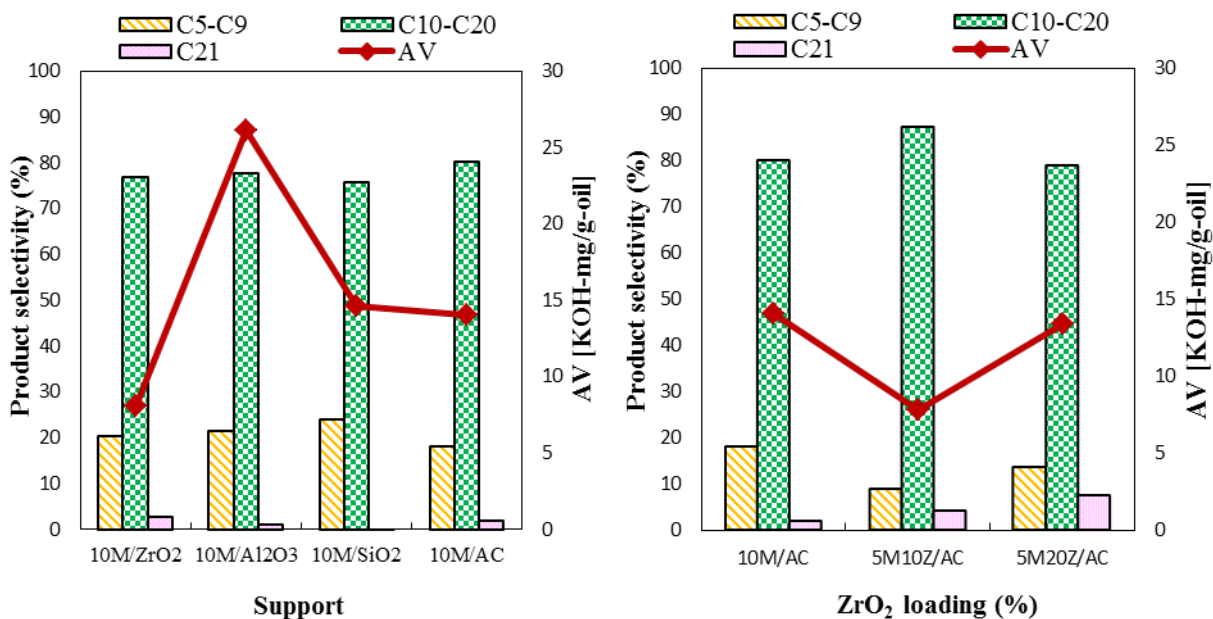
Figure 7: Product selectivity and acid value of the cracked oils

Figure 7 shows product selectivity and acid value of the cracked oils. From the results, 10M/ZrO$_2$ tended to give the lowest acid value followed by 10M/AC, 10M/SiO$_2$ and 10M/Al$_2$O$_3$, respectively, while the selectivity toward the product in diesel range hydrocarbons (C$_{10}$-C$_{20}$) was not significantly different for all catalysts. As the

ZrO_2 loading of 10wt%, the acid value decreased to 7.779 KOH-mg/g-oil since the oxygen vacancies of ZrO_2 adsorbed carboxylic acid molecules to form carboxylate species. The selectivity to diesel range hydrocarbons was also higher to 87% in accompanied with the decrease of 9% selectivity to gasoline range hydrocarbons. C_{21} compounds were found to be ketones as described above **(Scheme 1)** such as methyl ketone and ethyl ketone. By comparison, yield of these compounds on $10M/ZrO_2$ catalyst were higher than other catalysts. It was also found that the selectivity to C_{21} compounds increased with increasing ZrO_2 loading. This was consistent with the literatures that ZrO_2 was the active component for the ketonization of carboxylic acids [27].

4. Conclusion

In this work catalytic decarboxylation of waste cooking oil for the production of new hydrocarbon biodiesel over MgO-based catalysts supported on four types of support material (γ-alumina, silica, active carbon and zirconium oxide) was studied. All catalysts can convert triglycerides into deoxygenated biodiesel (C_{10}-C_{20}). The main products obtained from all catalysts were C_{15} and C_{17} hydrocarbons, the highest yield was observed for the 10M/AC catalyst. The 10M/AC catalyst became much more active and selective to diesel hydrocarbons production after ZrO_2 loading with 10wt%, and reduced the carbon formation on the catalyst surface. Thus, MgO-ZrO_2 on active carbon may be regarded as the promising decarboxy-cracking catalyst for synthesis HiBD from waste cooking oil.

Acknowledgements

References

[1] D.Y.C Leung, X. Wu and M.K.H Leung. "A review on biodiesel production using catalyzed transesterification." *Applied Energy*, vol. 87(4), pp. 1083-1095, Apr. 2010.

[2] M.P. Sharma. and G. Dwivedi "Cold flow behavior of biodiesel-A-review." International Journal of Renewable Energy Research, vol. 3, pp. 827-836, Dec. 2013.

[3] G. Dwivedi and M.P. Sharma. "Impact analysis of biodiesel on engine performance-A review." Renewable and Sustainable Energy Review, vol. 15, pp. 4633-4641, Dec. 2011.

[4] O.I. Senol, T.R. Viljava and A.O.I. Krause "Hydrodeoxygenation of aliphatic esters on sulphided NiMo/γ-Al_2O_3 and CoMo/γ-Al_2O_3 catalyst: The effect of water." Catalysis Today, vol. 106, pp. 186-189, Nov. 2005.

[5] O.I. Senol, E.M. Ryymin, T.R. Viljava and A.O.I. Krause "Reactions of methyl heptanoate hydrodeoxygenation on sulphided catalysts." Journal of Molecular Catalysis A: Chemical, vol. 268, pp. 1-8, May. 2007.

[6] O.I. Senol, T.R. Viljava and A.O.I. Krause "Effect of sulphiding agents on the hydrodeoxygenation of aliphatic esters on sulphided catalysts." Applied Catalysis A: General, vol. 326, pp. 236-244, Jul. 2007.

[7] J.G. Na, B.E. Yi, J.N. Kim, K.B. Yi, S.Y. Park, J.H. Park, J.N. Kim and C.H. Ko "Hydrocarbon production from decarboxylation of fatty acid without hydrogen." Catalysis Today, vol. 156, pp. 44-48, Oct. 2010.

[8] M. Snare, P. Maki-Arvela, I.L. Simakova, J. Myllyoja and D.Y. Murzin, "Overview of Catalytic Methods for Production of Next Generation Biodiesel from Natural Oils and Fats." Russian Journal of Physical Chemistry B, vol. 3, pp. 1035-1043, Dec. 2009.

[9] I. Simakova, O. Simakova, P. Maki-Arvela, A. Simakov, M. Estrada, and D.Y. Murzin, "Deoxygenation of palmitic and stearic acid over supported Pd catalysts: effect of metal dispersion." Applied Catalysis A: General, vol. 355, pp. 100-108, Feb. 2009.

[10] S. Lestari, P. Maki-Arvela, I. Simakova, J. Beltramini, G.Q.M. Lu, and D.Y. Murzin, "Catalytic Deoxygenation of Stearic Acid and Palmitic Acid in Semibatch Mode." Catalysis Letters, vol. 130, pp. 48-51, Jun. 2009.

[11] S. Lestari, P. Maki-Arvela, H. Bernas, O. Simakova, R. Sjoholm, J. Beltramini, G.Q.M. Lu, J. Myllyoja, I. Simakova, and D.Y. Murzin, "Catalytic Deoxygenation of Stearic Acid in a Continuous Reactor over a Mesoporous Carbon-Supported Pd Catalyst." Energy & Fuels, vol. 23, pp. 3842-3845, Aug. 2009.

[12] M. Snare, I. Kubickova, P. Maki-Arvela, D. Chichova, K. Eranen, and D.Y. Murzin, "Catalytic deoxygenation of unsaturated renewable feedstocks for production of diesel fuel hydrocarbons." Fuel, vol. 87, pp. 933-945, May. 2008.

[13] P. Maki-Arvela, M. Snare, K. Eranen, J. Myllyoja, and D.Y. Murzin, "Continuous decarboxylation of lauric acid over Pd/C catalyst." Fuel, vol. 87, pp. 3543-3549, Dec. 2008.

[14] S. Lestari, I. Simakova, A. Tokarev, P. Maki-Arvela, K. Eranen, and D.Y. Murzin, "Synthesis of biodiesel via deoxygenation of stearic acid over supported Pd/C catalyst." Catalysis Letters, vol. 122, pp. 247-251, May. 2008.

[15] M. Snare, I. Kubickova, P. Maki-Arvela, K. Eranen, J. Warna, and D.Y. Murzin, "Production of diesel fuel from renewable feeds: kinetics of ethyl stearate decarboxylation." Chemical Engineering Journal, vol. 134, pp. 29-34, May. 2007.

[16] P. Maki-Arvela, I. Kubickova, M. Snare, K. Eranen, and D.Y. Murzin, "Catalytic deoxygenation of fatty acids and their derivatives." Energy & Fuels, vol. 21, pp. 30-41, Jan. 2007.

[17] P. Maki-Arvela, I. Kubickova, M. Snare, K. Eranen, and D.Y. Murzin, "Heterogeneous catalytic deoxygenation of stearic acid for production of biodiesel." Industrial & Engineering Chemistry Research, vol. 45, pp. 5708-5715, Aug. 2006.

[18] I. Kubickova, M. Snare, K. Eranen, P. Maki-Arvela, and D.Y. Murzin, "Hydrocarbons for diesel fuel via decarboxylation of vegetable oils." Catalysis Today, vol. 106, pp. 197-200, Oct. 2005.

[19] J.G. Immer, M.J. Kelly and H.H. Lamb, "Catalytic reaction pathways in liquid-phase deoxygenation of C18 free fatty acids." Applied Catalysis A: General, vol. 375, pp. 134-139, Feb. 2010.

[20] T.A. Foglia and P.A. Barr, "Decarbonylation Dehydration of Fatty Acids to Alkenes in the Presence of Transition Metal Complexes." Journal of the American Oil Chemists Society, vol. 53, pp. 737-741, Dec. 1976.

[21] W.F. Maier, W. Roth and I. Thies, "Hydrogenolysis, IV. Gas Phase Decarboxylation of Carboxylic Acids." Chemische Berichte, vol. 115, pp. 808-812, Feb. 1982.

[22] H. Tani, M. Hasegawa, K. Asami and K. Fujimoto, "Selective Catalytic Decarboxy-Cracking of Triglyceride to Middle Distillate Hydrocarbon." Catalysis Today, vol. 164, pp. 410-414, Apr. 2012.

[23] H. Tani, M. Shimouchi, M. Hasegawa and K. Fujimoto, "Development of Direct Production Process of Diesel Fuel from Vegetable oils." Journal of the Japan Institute of Energy, vol. 90, pp. 466-470, May. 2011.

[24] P. Natewong, Y. Murakami, H. Tani and K. Asami, "Development of Heterogeneous Basic Catalysts Supported on Silica for the Synthesis of High Quality Bio-Diesel from Waste Cooking Oil." Journal of the Japan Institute of Energy, vol. 94, pp. 1393-1393, Aug. 2015.

[25] A. Zhang, Q. Ma, K. Wang, X. Liu, P. Shuler and Y. Tang, "Naphthenic acid removal from crude oil through catalytic decarboxylation on magnesium oxide." Applied Catalysis A: General, vol. 303, pp. 103-109, Apr. 2006.

[26] Y. Sun and C. Yang, "Properties Analysis of Spent Commercial Residue Hydrotreating Catalyst: Surface Property Changes of Spent Catalysts in Commercial Residue Hydrotreating Unit." Energy Science and Technology, vol. 6, pp. 67-72, Sep. 2013.

[27] T.N. Pham, T. Sooknoi, S.P. Crossley and D.E. Resasco, "Ketonization of Carboxylic Acids: Mechanisms, Catalysts, and Implications for Biomass Conversion." ACS Catalysis, vol. 3, pp. 2456-2473, Sep. 2013.